HHS Public Access

Author manuscript

Biofabrication. Author manuscript; available in PMC 2017 November 28.

Published in final edited form as:

Biofabrication. ; 7(3): 031001. doi:10.1088/1758-5090/7/3/031001.

In situ patterned micro 3D liver constructs for parallel toxicology testing in a fluidic device

Aleksander Skardal[1,2,3], **Mahesh Devarasetty**[1,2], **Shay Soker**[1,2,3], and **Adam R Hall**[1,2,3]

[1]Wake Forest Institute for Regenerative Medicine, Wake Forest Baptist Health, Medical Center Boulevard, Winston-Salem, NC 27157, USA

[2]Virginia Tech-Wake Forest University School of Biomedical Engineering and Sciences, Wake Forest Baptist Health, Medical Center Boulevard, Winston-Salem, NC 27157, USA

[3]Comprehensive Cancer Center, Wake Forest Baptist Health, Medical Center Boulevard, Winston-Salem, NC 27157, USA

Abstract

3D tissue models are increasingly being implemented for drug and toxicology testing. However, the creation of tissue-engineered constructs for this purpose often relies on complex biofabrication techniques that are time consuming, expensive, and difficult to scale up. Here, we describe a strategy for realizing multiple tissue constructs in a parallel microfluidic platform using an approach that is simple and can be easily scaled for high-throughput formats. Liver cells mixed with a UV-crosslinkable hydrogel solution are introduced into parallel channels of a sealed microfluidic device and photopatterned to produce stable tissue constructs *in situ*. The remaining uncrosslinked material is washed away, leaving the structures in place. By using a hydrogel that specifically mimics the properties of the natural extracellular matrix, we closely emulate native tissue, resulting in constructs that remain stable and functional in the device during a 7-day culture time course under recirculating media flow. As proof of principle for toxicology analysis, we expose the constructs to ethyl alcohol (0–500 mM) and show that the cell viability and the secretion of urea and albumin decrease with increasing alcohol exposure, while markers for cell damage increase.

Keywords

hydrogel; photopolymerization; toxicology; fluidic devices; tissue engineering

1. Introduction

The current drug development pipeline is long and expensive, often requiring nearly 15 years and upwards of $1 billion to develop a single commercialized compound. Unfortunately, due to the limitations of traditional testing approaches, drug compounds can reach the late stages of development, or even clinical use, before unpredicted toxicities in the

Supplementary material for this article is available online

The authors have no conflicts of interest to disclose.

human population or subpopulations are observed, thus rendering the drugs less efficient or even unusable. When they arise, these unintended consequences generally occur because the drug candidates in question were never robustly tested in human-specific models that sufficiently recapitulate the tissues and organs of the human body.

In the initial stages of drug development, candidate compounds are tested at high-throughput using cells of a target tissue type. Typically, this is performed in static, 2D monolayers of cells [1]. Although this is the conventional method for testing new compounds and has resulted in a vast number of discoveries, the process is fraught with difficulty; cells require unique microenvironmental cues to function and perform as they would *in vivo* and this complex microstructure cannot be replicated in 2D cultures. Techniques to reintroduce cultured cells into a more physiological environment utilize 3D culture systems such as cellular suspensions, rotating wall vessel bioreactors, scaffolds, and polymeric hydrogels [2]. 3D systems allow the development of cell–cell and cell–matrix interactions, localized hypoxia, and diffusion characteristics that are not possible in 2D cultures but are inherent in physiological tissue [3–5]. Without these factors, cells in 2D are phenotypically altered from their *in vivo* state [6]. As a result, improvements in 3D systems will consequently improve experimental efficacy; 3D *in vitro* systems integrating human cells could be used to predict *in vivo* response without the need for immunosuppression, thus enabling high-throughput and even personalized drug development.

Advances in microfluidic technology hold great potential for parallel tissue screening and dosing analysis. Microfluidic devices can be fabricated rapidly using standard polydimethylsiloxane (PDMS) molding techniques [7, 8] and can offer fluid delivery, mixing, and segregation in a self-contained system. However, integration of 3D tissue constructs (organoids) in the platform can be challenging. Biofabrication techniques like cell encapsulation [9] and bioprinting [10, 11] are valuable, but require extensive equipment and may present challenges in scaling up to massively parallel detection schemes due to their serial nature. An alternative approach with great potential is patterned photopolymerization. Photocrosslinkable precursor materials can be introduced selectively to microfluidic chambers using their intrinsic fluid exchange capabilities and external photopatterning can be easily integrated to produce structures *in situ*.

While photopatterning has been used to produce biologically-relevant structures [12] and even simple constructs containing living cells [13–15], recapitulation of physiological tissue behavior and long-term cell viability has been limited. In past work, either non-cell adherent polyethylene glycol-based polymers or highly cell-adherent Type I collagen has been used, neither of which faithfully reproduces the complex nature of the natural extracellular matrix (ECM). Here, we use a hyaluronic acid (HA) and gelatin-based hydrogel to mimic the native ECM in photopatterned tissue constructs *in situ*. This modular hydrogel system is designed to more fully replicate the complexity of the native ECM. HA provides an ECM-like structure in the form of crosslinked HA polysaccharide chains and cell-adherent motifs in the form of hydrolytically degraded collagen gel [16]. Importantly, we also incorporate into the hydrogel a solution derived directly from the liver ECM, presenting encapsulated cells with additional collagens, glycosaminoglycans, elastin, and growth factors specific to the liver [17]. In total, this material provides the most accurate mimic of native tissue currently

available. We employ a single-step fabrication process to produce multiple, identical human liver-based tissue constructs in the parallel chambers of a microfluidic device using this ECM mimic. We show that these constructs can be maintained long-term (for at least 7 days) and demonstrate proof-of-principle *in situ* toxicology screening using alcohol exposure as a model.

2. Materials and methods

2.1. Fluidic device fabrication

The device consists of four circular chambers (10 mm diameter, 3 mm thick), each accessible via a separate fluidic channel with an individually addressable inlet and outlet (figure 1(a)). These structures are fabricated using conventional soft lithography and replica molding [18]. Briefly, an inverted channel structure is produced using 3D printing (Zprinter 450, Z Corp., Rock Hill, SC) and used as a mold for device definition. Polydimethylsiloxane (PDMS, Sylgard 184, Dow Corning, Midland, MI) is mixed thoroughly with its curing agent and degassed before being poured directly onto the mold and cured at 60 °C for 60 min in an oven. Following curing, the device is isolated using a razor and removed from the mold. After cleaning, the bottom of the device is dip-coated with uncured PDMS and positioned on a clean glass slide, where it is cured under mild pressure at 90 °C for 10 min on a hot plate, sealing the device permanently. The PDMS and glass devices are sterilized by autoclaving and stored sterile prior to use in cell-based studies. Fluidic connections are made using stainless steel catheter couplers (Instech Laboratories, Inc., Ply-mouth Meeting, PA) and Sylastic tubing (Dow Corning, Midland, MI).

2.2. *In situ* liver construct biofabrication by photo-patterning

HEPG2 hepatoma cells (ATCC, Manassas, VA) are expanded in 2D on tissue culture plastic using 15 cm tissue-treated dishes (Corning Inc., Corning, NY) until 90% confluence with Dulbecco's Minimum Essential Medium (DMEM, Hyclone, Logan, UT) containing 10% fetal bovine serum (FBS, Hyclone). HEPG2 cells do not possess the same level of functionality as primary hepatocytes, but do retain some aspects of liver function, and are an appropriate choice for demonstrating biofabrication techniques and simple toxicology screens. Cells are harvested using Trypsin/EDTA (Hyclone) before further use. In order to form the liver ECM-mimicking HA/gelatin-based hydrogel (HyStem-HP, ESI-BIO, Alameda, CA), the thiolated HA component (Glycosil) and the thiolated gelatin component (Gelin-S) are dissolved in sterile water containing 0.1% w/v of the photoinitiator 4-(2-hydroxyethoxy)phenyl-(2-propyl)ketone (Sigma St. Louis, MO) to make 2% w/v solutions. The polyethylene glycol diacrylate (PEGDA) crosslinker (Extralink, ESI-BIO) is dissolved in the photoinitiator solution to make a 4% w/v solution. Glycosil, Gelin-S, and Extralink are then mixed in a 2:2:1 ratio by volume, and in turn mixed in a 1:1 ratio by volume with liver ECM-derived solution as described elsewhere [17]. The resulting solution is vortexed and used to resuspend the HEPG2 cells at a cell density of 5 million cells mL^{-1}. This hydrogel precursor–cell mixture is introduced into each of the device channels using the prefabricated inlet ports (figure 1(b(i–ii))). The construct position is then defined in each chamber by UV exposure (365 nm, 18 W cm^{-2}) for 5 s through a printed transparency photomask with apertures of 4 mm diameter (figure 1(b(iii))) to initiate a thiol–ene stepwise

crosslinking reaction, resulting in HEPG2 cells that are encapsulated within the patterned hydrogel regions of 4 mm diameter (figure 1(b(iv))). After crosslinking, the remaining precursor–cell mixture is flushed from the device using PBS, leaving a cylindrical HEPG2 liver construct within each chamber of the device (figure 1(b(v))). The results described here are performed in triplicate using three separate parallel fluidic devices.

2.3. Operation of devices for construct culture and alcohol insult

Medium flow is introduced to each segregated channel of the fluidic device, resulting in 4 parallel chambers per chip. Sylastic tubing is used to connect media reservoirs to a MP2 Precision micro-peristaltic pump (Elemental Scientific, Inc., Omaha, NE). Additional tubing further connects the pump to the device channels, and back to the reservoirs, forming closed parallel circuits (figure 2(a)). At the start of culture, 4 mL of medium (DMEM, Lonza) was placed in each reservoir, after which fluid flow was initiated by the micro-peristaltic pump. To achieve alcohol insult, each fluidic channel is subjected to a medium preparation spiked with a different ethanol concentration (0 mM, 50 mM, 100 mM, and 500 mM). Medium flow is maintained at a rate of 5 μL min^{-1} throughout the experiment. An aliquot from each reservoir is removed daily and frozen at −80 °C for analysis. The reservoir solution is then replaced with clean medium containing the same ethanol concentration. Devices are operated continuously for 7 days.

2.4. Assessment of liver function

Secreted levels of albumin in 100 μL aliquots are quantified using a Human Albumin ELISA Kit (Alpha Diagnostic International, San Antonio, TX). Quantification is performed on a Spectramax M5 plate reader (Molecular Devices, Sunnyvale, CA) at 450 nm. Secreted levels of urea in 100 μL aliquots are quantified using a QuantiChrom™ Urea Colorimetric Assay Kit (BioAssay Systems, Hayward, CA). Quantification is performed on the plate reader at 430 nm.

2.5. Assessment of cell viability and cytotoxicity

Cell viability is assessed by two independent measurements: LIVE/DEAD (L/D) staining and quantification of alpha glutathione-S-transferase (αGST), a liver biomarker that is released from liver cells upon cell death and lysis. L/D staining is performed on day 7 at the end of the culture period. Medium is flushed from the device channels manually using PBS and the viability is determined using the L/D Viability/Cytotoxicity Kit for mammalian cells (Life Technologies, Grand Island, NY). Concentrations of 2 μM calcein-AM and 4 μM ethidium homodimer-1 in a 1:1 mixture of PBS and DMEM are prepared for the assay and introduced into the device construct chambers. Constructs are incubated with the solution for 60 min, after which they are fixed with 4% paraformaldehyde for 60 min and washed with PBS. The constructs are imaged *in situ* using a Leica TCS LSI macro-confocal microscope. Z-stacks of 150 μm are taken of each construct, from which maximum projections (2D compressed image) and 3D reconstructions are obtained. Viability is calculated from the cells visible in the maximum projections by determining the percentage of viable cells relative to the total number of cells. αGST levels are analyzed daily using the media aliquots taken during the 7-day culture time course and quantified using a Glutathione S-Transferase

Alpha ELISA Assay Kit (Oxford Biomedical Research, Oxford, MI). Quantification is performed on a plate reader at 430 nm.

2.6. Statistical analysis

The data are generally presented as the means of number of replicates ± the standard deviation. All experiments were performed with $n = 3$ or higher. Values were compared using Student's *t*-test (2-tailed) with two sample unequal variance, and $p < 0.05$ or less was considered statistically significant.

3. Results and discussion

3.1. Device design and construct biofabrication

Standard soft lithography and replica molding techniques were employed to generate a set of devices, each consisting of four circular chambers (10 mm diameter, 3 mm thick) independently accessible via separate fluidic channels (figure 1(a)). The devices were bonded to standard microscope slides, enabling standard imaging procedures to be performed during the study. After sealing, we confirmed that fluid flow could be maintained for a range of flow rates (1–25 μL min^{-1}) for days without evidence of leaks or clogged circuits.

HA hydrogels crosslinked by PEGDA have been implemented in numerous applications in tissue engineering and regenerative medicine, including wound healing [19, 20], post-surgical adhesion production [21], biofabrication of tissue constructs [22–24] and tissue spheroids [25], and in tissue specific environments for primary cell cultures [17]. Recently, we modified this hydrogel system to provide extremely fast gelation kinetics [26], allowing for efficient tissue organoid construction with improved spatial control over polymerization zones, while maintaining hydrogel properties such as the pore size and elastic modulus of the original non-photocrosslinkable version (Supp. figures 1(a), (b)), which have proven appropriate for 3D tissue cultures. The unique combination of faithful ECM mimicry with high photosensitivity makes this material an ideal platform for *in situ* tissue construct formation. Few materials mimic the native ECM and support the addition of bioactive factors, and are also highly adaptable to multiple biofabrication techniques. This system is comprised of naturally-derived materials that are native to the body. Additionally, our HA/gelatin system also supports the modular addition of additional ECM factors, such as cytokines and growth factors [17], if desired, via heparin-modulated binding, thereby increasing its biomimetic properties compared to other photopolymerizable materials such as PEGDA and methacrylated gelatin. The true benefit with respect to the work described here is the capability of this hydrogel system to support on-demand photopolymerization with zonal discrimination. This allows encapsulation of cells in 3D only upon UV light exposure, and limits the crosslinking and hydrogel formation to only those regions exposed. This capability is not supported by more traditional gel materials with slow crosslinking kinetics, such as collagen Type I and Matrigel, or fast, but more difficult to control kinetics, such as alginate, making these materials less effective for biofabrication (Supp. figure 1(c)).

Figure 1(b(vi)) shows a typical device following the biofabrication procedure with four patterned HEPG2 constructs, each formed in an individually addressable fluidic chamber. We find that these constructs are mechanically robust even under significant flow (>30 μL min^{-1}), indicating that they are strongly adhered to the top and bottom of the chamber (PDMS and glass, respectively).

We found high cell viability in liver constructs exposed to normal media, even after 7 days of culture, as shown by L/D staining and confocal microscopy (figure 2(b)). Quantification of viable and dead cells using maximum intensity projection images (Supplemental figure 2(a)) from these confocal data yield an average viability of >75% (figure 2(f)). This demonstrates that the fluidic device is capable of sustaining the liver constructs long-term. Some cell death is observed at the core of the construct, which we attribute to the limited availability of nutrients to the core of the patterned structure. This can be addressed by scaling down the construct volume (c.f. figure 4(c)).

Using ELISA (figure 3(a)), we observe a constant albumin level of approximately 8 ng mL^{-1} for the 0 mM ethanol control group. This represents steady-state production for a healthy construct under these conditions. In addition, we also analyze the urea concentration using a colorimetric assay (figure 3(b)). Urea is synthesized by liver cells as a result of the metabolism of nitrogen-containing compounds and is therefore another natural target for analysis of the HEPG2 construct function. We observe a consistent level of urea production in the 0 mM ethanol control group, remaining at approximately 18 ng mL^{-1} for the duration of the experiment (from day 2 on), qualitatively similar to albumin. Collectively, these baseline data demonstrate that the device conditions can successfully maintain liver construct viability and function for at least a 7-day period of time.

3.2. Effects of ethanol insult on liver construct viability and function

To demonstrate the ability of our system to assess the viability and function of the liver constructs, we perfused parallel constructs with DMEM spiked with 0 mM, 50 mM, 100 mM, or 500 mM ethanol. From L/D imaging (day 7, figures 2(b)–(e)), we find a dose-dependent impact on viability, qualitatively validating the assay; as ethanol concentration is increased, the number of viable cells decreases sharply, with no observable viability at 500 mM. This trend is supported by quantification of viability (% live cells/total cell number), which shows a statistically significant decrease in the percent of viable cells with each increase in ethanol concentration ($p < 0.05$, figure 2(f)). We note that overall L/D cell staining was decreased somewhat at the center of the constructs. We attribute this observation to decreased availability of oxygen and nutrients at the hydrogel core. As a result, cells in the central region are likely to have died early or migrated towards the perimeter of the constructs. Still, this would result in a systematic error that would not affect our conclusions. Future miniaturization of constructs will mitigate these limitations.

We used the media aliquots collected daily during culture to measure the levels of secreted albumin across the range of ethanol concentrations (figure 3(a)). Using ELISA, we observed a constant albumin level of approximately 8 ng mL^{-1} for the 0 mM ethanol control group. Albumin concentrations were significantly lower for all ethanol-exposed groups from day 3 through day 7 ($p < 0.05$), indicating reduced cell functionality. We found that albumin

production decreased for these samples throughout the culture time in a manner that appears weakly dose dependent, although the albumin levels in the three ethanol exposure concentrations are not significantly different from each other.

Colorimetric analysis of urea concentration (figure 3(b)) showed a consistent level of urea production in the 0 mM ethanol control group, remaining at approximately 18 ng mL^{-1} for the duration of the experiment (from day 2 on). However, as ethanol concentration was increased, we observed a consistent dose dependent decrease in production, with the control group urea level significantly higher than those of the other groups from day 4 on ($p < 0.05$). The three ethanol-exposed groups were not significantly different from one another at each time point, but the concentration-dependent trend is evident from the data.

To further assess the ethanol toxicity, we measure the amount of αGST released from the liver constructs as a function of time and ethanol exposure. αGST is an enzyme catalyst that is used to conjugate glutathione to substances in the liver during detoxification. It occurs naturally in hepatocytes and hepatocyte-derived cells, such as the HEPG2 cells employed in this study. When cell death occurs by apoptosis and the cell membrane lyses, αGST is released into the surrounding milieu. As such, it is a useful soluble biomarker for monitoring cell death during toxic injury to the liver. Using ELISA (figure 3(c)), we find that αGST in the 0 mM ethanol control group remains low consistently throughout the study, never accumulating above 1 ng mL^{-1} during any 24 h period in the study. This result is consistent with the high viability observed for the same control group through L/D staining at the end of the 7 day study. Conversely, the most toxic condition of 500 mM ethanol results in high αGST levels immediately on day 1 (24 h after fabrication), suggesting acute cell death and subsequent cell lysis. With few viable cells left in the constructs, αGST levels quickly drop after day 2, remaining near zero for the remainder of the study. The 50 mM and 100 mM groups display a more complicated behavior. In both groups, αGST levels are elevated compared to the control sample on day 1, but not to the degree at which it is observed in the 500 mM ethanol group ($p < 0.05$). αGST then reduces somewhat until days 5 and 6, at which point levels significantly increase compared to previous time points ($p < 0.05$) with a more pronounced increase in the higher concentration (100 mM ethanol) group. We interpret these data to indicate a long-term (chronic) influence of ethanol dosage on the constructs. Intermediate ethanol concentrations are more toxic than the control condition immediately, but require time to induce the net toxicity observed by L/D analysis. On days 5 and 6, the 100 mM condition results in a significantly increased αGST concentration ($p < 0.05$) in the media compared to the control and to the 50 mM condition (on day 6). The reasons for this spike are currently under study, but may be the result of temporary dilution of the ethanol concentration internal to the construct by dead and lysed cells at the perimeter.

Collectively, these data are indicative of progressive cell death; as the ethanol concentration increases, so too does toxicity (αGST), causing cell function (including albumin and urea production) to be limited. This quantification is therefore a direct measure of the cell viability throughout the experiment. Notably, the 0 mM control group produced a relatively consistent secretion level, confirming that these HEPG2-based liver constructs retained sufficient liver function for use in this study. We recognize the limitations of HEPG2 cells, and are transitioning to liver constructs comprised of primary human hepatocytes and other

supportive cell types. In future studies, implementation of these primary human hepatocytes will yield a higher level of function, including drug metabolism capabilities, resulting in a more effective model [27]. Nevertheless, the differences in quantitative albumin and urea data between ethanol conditions clearly demonstrate the efficacy of this device platform to be used in toxicology screening, with enough specificity for quantitative biochemical analysis.

It should also be noted that HEPG2 cells can behave differently in 3D than on 2D tissue culture plastic, potentially increasing their function, and usefulness for *in vitro* models. In fact, it has been shown that simply transitioning from 2D to 3D resulted in increased HEPG2 albumin expression and secretion [28]. This is not limited to HEPG2s either. INT407 cells, an intestine epithelial cell line, fails to secrete significant levels of mucins in 2D, but when transitioned to 3D aggregate cultures, mucin production and secretion increased significantly [29]. We show in Supp. Figure 3 that 2D culture on tissue culture plastic results in a proliferative state (significant increases in MTS assay absorbance readings over time), but that when placed in a 3D culture (our photopolymerizable HA hydrogel or a standard collagen Type I gel), proliferation rates slow. This slowed rate of proliferation places these cells more in line with hepatocyte cultures, which do not proliferate. That being said, hepatocytes are the industry standard for *in vitro* testing, but the biological component we employed in this study was sufficiently functional to demonstrate the usefulness of the biofabrication approach and the subsequent ability to perform screening studies with the system.

Together these data agree qualitatively and quantitatively with expectations, and importantly validate the concept, design, and implementation of our system for *in situ* toxicology screening of tissue constructs in a microfluidic device. We anticipate that similar results can be achieved in studies assessing other sources of liver toxicity, such as potent chemotherapeutic agents. The system also enables the creation of constructs of different tissue types, as well as the series connection of multiple tissue types for an integrated systems biology ‘body-on-a-chip’ approach to toxicology and drug screening.

Parallel studies using traditional 2D cell cultures were not included here because differences in sample volume and diffusion characteristics make quantitative comparison between 2D and 3D cultures difficult. However, the advantages of 3D culture for reproducing *in vivo* environments have been reported extensively. For example, primary human hepatocytes cultured in 3D HA hydrogels with liver ECM components outperform parallel cultures on plastic and collagen in viability, mitochondrial metabolism, albumin production, and drug metabolism [17]. In other tissue types, researchers have demonstrated that epithelial cells from the intestine, colon, and lung were shown to display *in vivo*-like characteristics in 3D formats, such as the expression of polarity markers, enhanced expression of cell–cell adhesion markers, ECM proteins, and localized mucin production [29–33]. Furthermore, 3D tumor models have shown effectiveness as models for *in vivo* conditions [4, 5].

3.3. System size scale down for future high-throughput parallelization

Scaling down construct size will enable high-throughput device systems, thus increasing statistical power. Future studies will employ such systems to increase the number of

experimental conditions probed per device. To demonstrate the ability of our biofabrication technique as a viable option for system scale-down, we now repeat the *in situ* gel polymerization method using a photomask composed of circular patterns with various diameters. Hydrogel precursor solutions are prepared as described above without cells, but containing a fluorescent dye (Alexa Fluor 488) that is covalently bound within the hydrogel network to illuminate the crosslinked constructs under the microscope. The hydrogels are patterned between parallel microscope slides with PDMS spacers to form a channel. Figures 4(a)–(c) show confocal micrographs of the resulting constructs, demonstrating that we are able to achieve functional constructs as small as 150 μm in diameter (figure 4(c)), limited only by diffraction of the UV source. This can be mitigated through control of the glass substrate thickness and reduction of the chamber height. Miniaturization will also decrease the distances within the tissue constructs through which nutrients and oxygen diffuse, thereby increasing the construct viability in future experiments.

4. Conclusion

We have demonstrated a microfluidic device featuring individually addressable tissue constructs photopatterned using an accurate mimic of the ECM. Constructs formed in this way can be maintained long-term (for at least 7 days) and allow active control of the solvent conditions throughout the experiment. To show efficacy for toxicological screening, we used this platform to successfully assess albumin and urea production, as well as αGST release, over a range of ethanol concentrations. We found that ethanol dosing from 0 to 500 mM results in a systematic effect on cell viability, as determined by L/D staining and toxicity-induced αGST release. Additionally, analytical assessment of liver function showed that the output of both human serum albumin and urea are significantly reduced under increasing ethanol exposure.

While parallelizing 3D tissue models is challenging with conventional biofabrication techniques, photo-patterning enables easy, large area fabrication of arbitrary arrays. Our choice of ECM mimic offers additional flexibility to the system as well. In the future, the material will also allow for a variety of modifications and manipulations, such as heparinization for growth factor immobilization [17], multiple crosslinking chemistries that can be performed in the presence of cells [9, 22, 26], and control over mechanical properties [24]. We expect that our overall approach will be useful in a wide range of applications that will benefit from the use of 3D models as opposed to traditional 2D cell cultures, including drug development, complex toxicology testing, and personalized medicine.

Supplementary Material

Refer to Web version on PubMed Central for supplementary material.

Acknowledgments

ARH acknowledges start-up funds from Wake Forest University School of Medicine. AS and ARH acknowledge funds from the Wake Forest Institute for Regenerative Medicine Promoting Innovating Discoveries Funding Program.

References

1. Hughes JP, Rees S, Kalindjian SB, Philpott KL. Principles of early drug discovery. Br J Pharmacol. 2011; 162:1239–49. [PubMed: 21091654]
2. Barrila J, et al. Organotypic 3D cell culture models: using the rotating wall vessel to study host-pathogen interactions. Nat Rev Microbiol. 2010; 8:791–801. [PubMed: 20948552]
3. Achilli TM, Meyer J, Morgan JR. Advances in the formation, use and understanding of multi-cellular spheroids. Expert Opin Biol Ther. 2012; 12:1347–60. [PubMed: 22784238]
4. Drewitz M, et al. Towards automated production and drug sensitivity testing using scaffold-free spherical tumor microtissues. Biotechnol J. 2011; 6:1488–96. [PubMed: 22102438]
5. Ho WJ, et al. Incorporation of multicellular spheroids into 3D polymeric scaffolds provides an improved tumor model for screening anticancer drugs. Cancer science. 2010; 101:2637–43. [PubMed: 20849469]
6. Baker BM, Chen CS. Deconstructing the third dimension: how 3D culture microenvironments alter cellular cues. J Cell Sci. 2012; 125:3015–24. [PubMed: 22797912]
7. McDonald JC, et al. Fabrication of microfluidic systems in poly(dimethylsiloxane). Electrophoresis. 2000; 21:27–40. [PubMed: 10634468]
8. Qin D, Xia Y, Whitesides GM. Soft lithography for micro- and nanoscale patterning. Nat Protoc. 2010; 5:491–502. [PubMed: 20203666]
9. Zhang J, Skardal A, Prestwich GD. Engineered extracellular matrices with cleavable crosslinkers for cell expansion and easy cell recovery. Biomaterials. 2008; 29:4521–31. [PubMed: 18768219]
10. Jakab K, et al. Tissue engineering by self-assembly of cells printed into topologically defined structures. Tissue Eng. 2008; A 14:413–21.
11. Murphy SV, Atala A. Organ engineering–combining stem cells, biomaterials, and bioreactors to produce bioengineered organs for transplantation. BioEssays: News and Reviews in Molecular, Cellular and Developmental Biology. 2013; 35:163–72.
12. Bischel LL, Lee SH, Beebe DJ. A practical method for patterning lumens through ECM hydrogels via viscous finger patterning. J Lab Autom. 2012; 17:96–103. [PubMed: 22357560]
13. Cheung YK, Gillette BM, Zhong M, Ramcharan S, Sia SK. Direct patterning of composite biocompatible microstructures using microfluidics. Lab Chip. 2007; 7:574–9. [PubMed: 17476375]
14. Gao D, Liu J, Wei HB, Li HF, Guo GS, Lin JM. A microfluidic approach for anticancer drug analysis based on hydrogel encapsulated tumor cells. Anal Chim Acta. 2010; 665:7–14. [PubMed: 20381684]
15. Koh WG, Revzin A, Pishko MV. Poly(ethylene glycol) hydrogel microstructures encapsulating living cells. Langmuir. 2002; 18:2459–62. [PubMed: 12088033]
16. Prestwich GD. Engineering a clinically-useful matrix for cell therapy. Organogenesis. 2008; 4:42–7. [PubMed: 19279714]
17. Skardal A, Smith L, Bharadwaj S, Atala A, Soker S, Zhang Y. Tissue specific synthetic ECM hydrogels for 3D *in vitro* maintenance of hepatocyte function. Biomaterials. 2012; 33:4565–75. [PubMed: 22475531]
18. Xia Y, Whitesides GM. Soft lithography. Annu Rev Mater Sci. 1998; 28:153–84.
19. Kirker KR, Luo Y, Morris SE, Shelby J, Prestwich GD. Glycosaminoglycan hydrogels as supplemental wound dressings for donor sites. J Burn Care Rehabil. 2004; 25:276–86. [PubMed: 15273469]
20. Kirker KR, Luo Y, Nielson JH, Shelby J, Prestwich GD. Glycosaminoglycan hydrogel films as bio-interactive dressings for wound healing. Biomaterials. 2002; 23:3661–71. [PubMed: 12109692]
21. Liu Y, Skardal A, Shu XZ, Prestwich GD. Prevention of peritendinous adhesions using a hyaluronan-derived hydrogel film following partial-thickness flexor tendon injury. J Orthop Res. 2008; 26:562–9. [PubMed: 17985390]
22. Skardal A, Zhang J, McCoard L, Oottamasathien S, Prestwich GD. Dynamically crosslinked gold nanoparticle—hyaluronan hydrogels. Adv Mater. 2010; 22:4736–40. [PubMed: 20730818]

23. Skardal A, Zhang J, McCoard L, Xu X, Oottamasathien S, Prestwich GD. Photocrosslinkable hyaluronan-gelatin hydrogels for two-step bioprinting. Tissue Eng. 2010; A 16:2675–85.
24. Skardal A, Zhang J, Prestwich GD. Bioprinting vessel-like constructs using hyaluronan hydrogels crosslinked with tetrahedral polyethylene glycol tetracrylates. Biomaterials. 2010; 31:6173–81. [PubMed: 20546891]
25. Skardal A, Sarker SF, Crabbe A, Nickerson CA, Prestwich GD. The generation of 3D tissue models based on hyaluronan hydrogel-coated microcarriers within a rotating wall vessel bioreactor. Biomaterials. 2010; 31:8426–35. [PubMed: 20692703]
26. Murphy SV, Skardal A, Atala A. Evaluation of hydrogels for bio-printing applications. J Biomed Mater Res. 2013; A 101:272–84.
27. Wilkening S, Stahl F, Bader A. Comparison of primary human hepatocytes and hepatoma cell line Hepg2 with regard to their biotransformation properties. Drug Metab Dispos. 2003; 31:1035–42. [PubMed: 12867492]
28. Matsuzawa A, Matsusaki M, Akashi M. Construction of three-dimensional liver tissue models by cell accumulation technique and maintaining their metabolic functions for long-term culture without medium change. J Biomed Mater Res. 2015; A 103:1554–64.
29. Honer ZU, et al. Three-dimensional organotypic models of human colonic epithelium to study the early stages of enteric salmonellosis. Microbes Infect. 2006; 8:1813–25. [PubMed: 16730210]
30. Carterson AJ, et al. A549 lung epithelial cells grown as three-dimensional aggregates: alternative tissue culture model for Pseudomonas aeruginosa pathogenesis. Infect Immun. 2005; 73:1129–40. [PubMed: 15664956]
31. Hjelm BE, Berta AN, Nickerson CA, Arntzen CJ, Herbst-Kralovetz MM. Development and characterization of a three-dimensional organotypic human vaginal epithelial cell model. Biol Reprod. 2010; 82:617–27. [PubMed: 20007410]
32. LaMarca HL, et al. Three-dimensional growth of extravillous cytotrophoblasts promotes differentiation and invasion. Placenta. 2005; 26:709–20. [PubMed: 16226120]
33. Nickerson CA, et al. Three-dimensional tissue assemblies: novel models for the study of Salmonella enterica serovar Typhimurium pathogenesis. Infect Immun. 2001; 69:7106–20. [PubMed: 11598087]

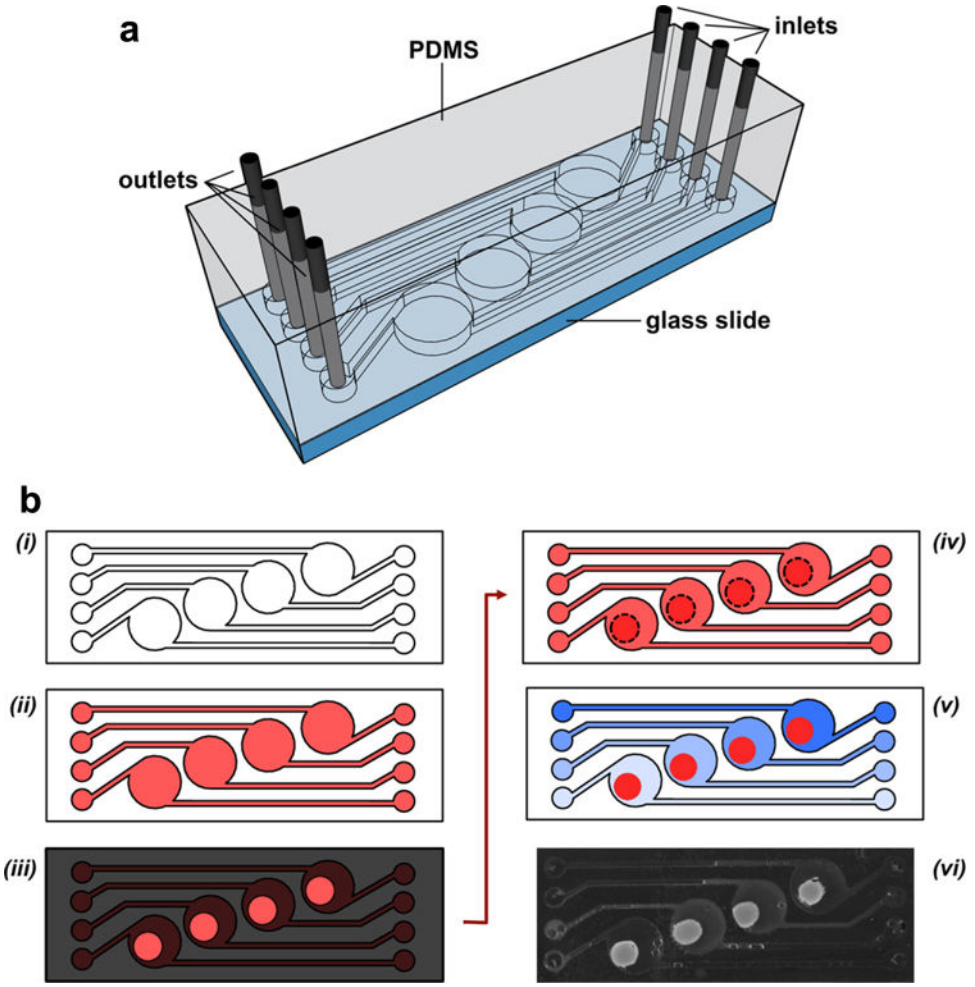

Figure 1.

(a) Schematic of the assembled device, showing four discrete chambers, each addressable by an inlet and outlet. (b) Workflow for construct formation in the fluidic device. All fluidic channels (i) are filled with a mixture of HEPG2 cells and the HA/PEGDA precursor (light red, ii). A printed transparency photomask (grey) is employed to define constructs (iii). Following UV exposure, cross-linked constructs (dashed lines) are formed in the channels (iv) and the remaining solution is replaced, first with clean PBS and then with the desired ethanol mixture (v). Epifluorescence imaging (vi) confirms construct formation.

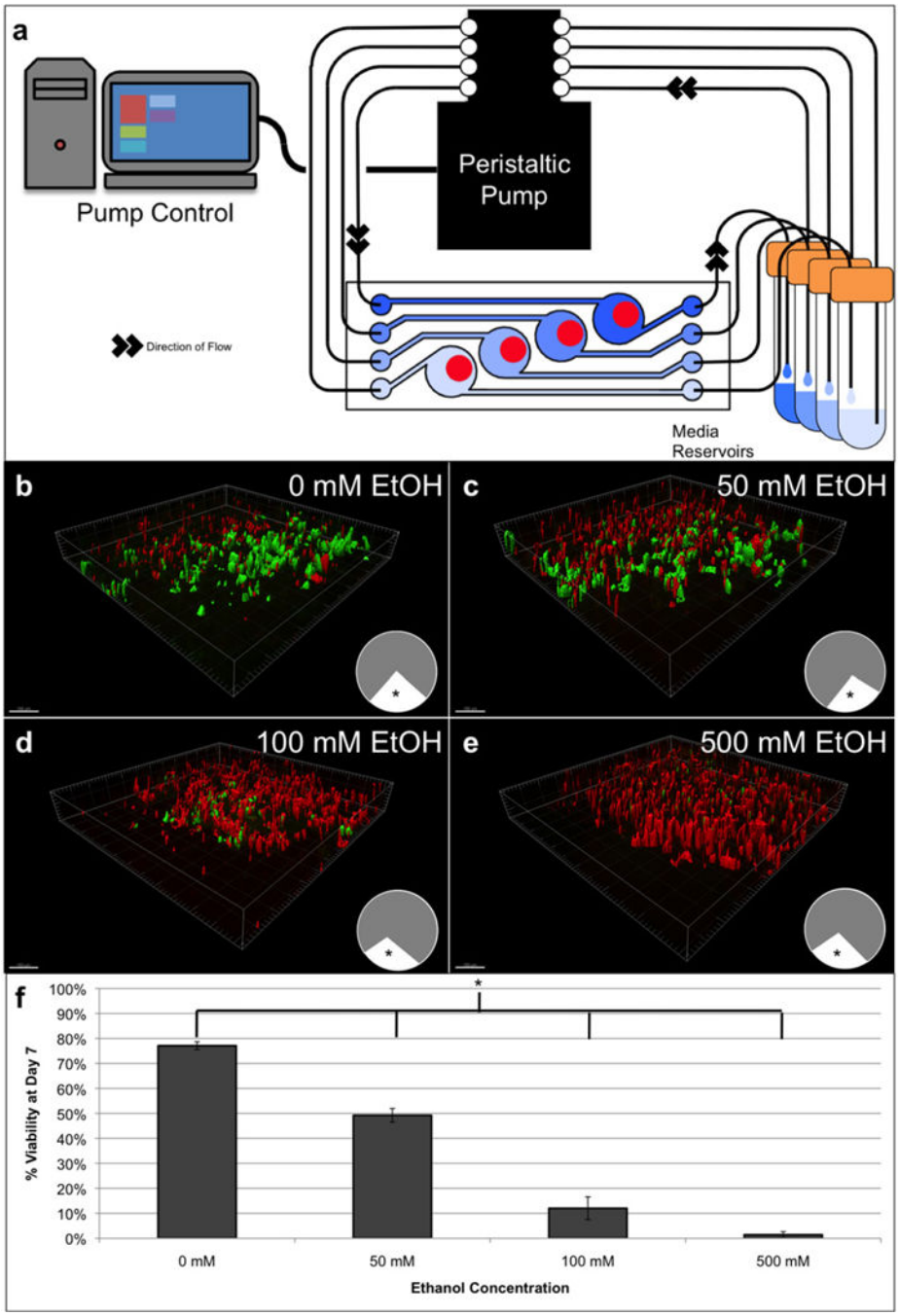

Figure 2.

(a) Schematic representation of ethanol toxicity measurement. Media containing increasing concentrations of ethanol are flowed continuously through the parallel chambers of the fluidic device using a computer-controlled peristaltic pump. (b)–(e) L/D analysis on day 7 of constructs exposed to the indicated ethanol (EtOH) concentration. Each image represents a 3D reconstruction of a 150 μm Z-stack of confocal images taken at the conclusion of the experiment (day 7). Green fluorescence indicates calcein AM-stained live cells and red fluorescence indicates ethidium homodimer-1-stained dead cells; Scale bar −250 μm. The

asterisk-indicated white region of the disk in each panel indicates the region of the organoid represented by the image. (f) Quantified cell viability percentages of constructs on day 7 at each ethanol concentration. (Significance: *$p < 0.05$ between all group-to-group comparisons.)

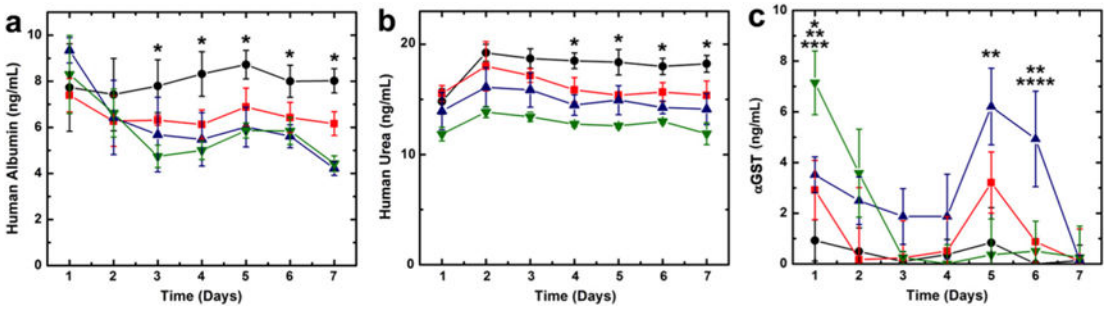

Figure 3.

Assessment of (a) human serum albumin, (b) urea concentrations, and (c) alpha glutathione-S-transferase in the presence of 0 mM (black circles), 50 mM (red squares), 100 mM (blue upward triangles), and 500 mM (green downward triangles) ethanol. Significance in (a), (b) * $p < 0.05$ between 0 mM and all other conditions. Significance in (c) * $p < 0.05$ between 0 mM and 500 mM; ** $p < 0.05$ between 0 mM and 100 mM; *** $p < 0.05$ between 50 mM and 500 mM, and between 100 mM and 500 mM; **** $p < 0.05$ between 50 mM an 100 mM.

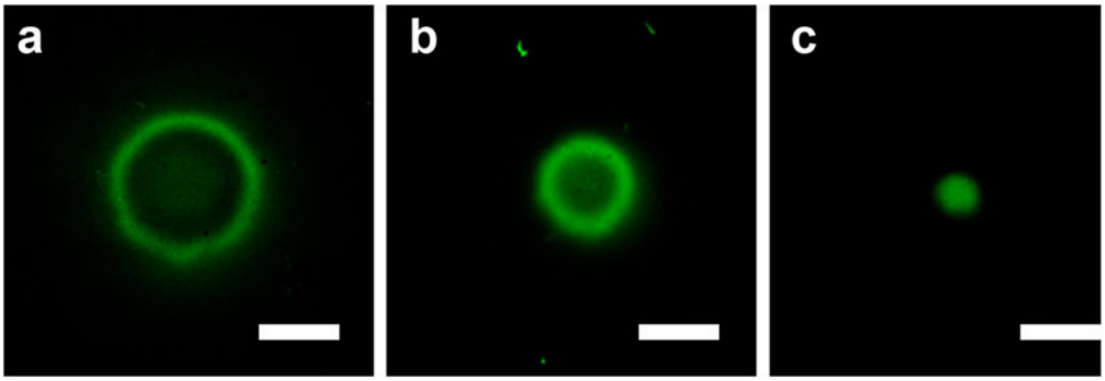

Figure 4.

Confocal micrographs of small, Alexa Fluor 488 labeled hydrogel constructs fabricated *in situ* in a fluidic chamber. Photomask diameters are (a) 500 μm, (b) 250 μm, and (c) 100 μm. All scale bars represent 400 μm.